Enhanced superconductivity and moderate spin fluctuations suppressed at low energies in heavily electron-doped La1111-based superconductor

T. Kouchi,[1,*] S. Nishioka,[1] K. Suzuki,[1] M. Yashima,[1] H. Mukuda,[1,†] T. Kawashima,[2]
H. Tsuji,[2] K. Kuroki,[2] S. Miyasaka,[2] and S. Tajima[2]
[1]*Graduate School of Engineering Science, Osaka University, Osaka 560-8531, Japan*
[2]*Graduate School of Science, Osaka University, Osaka 560-0043, Japan*

(Received 28 October 2021; revised 8 April 2022; accepted 8 April 2022; published 28 April 2022)

To elucidate the origin of the reenhanced high-T_c phase in the heavily electron-doped Fe pnictides, systematic ^{75}As NMR studies are performed on heavily electron-doped LaFePnO$_{0.75}$H$_{0.25}$ by controlling the pnictogen height (h_{Pn}) from the Fe plane through the substitution at Pn(= As) site with Sb or P. The measurements of nuclear spin relaxation rate ($1/T_1$) and Knight shift (K) reveal that the moderate spin fluctuations at high temperatures are suppressed toward low temperatures. Such characteristic spin fluctuations with gaplike feature at low energies are more enlarged in higher T_c compounds with higher h_{Pn}, while those are totally suppressed in nonsuperconducting compounds with lower h_{Pn}. This implies that the contribution of the finite-energy part in the spin-fluctuation spectrum is crucial for enhancing T_c in the heavily electron-doped regime. This is in contrast to many cases of typical Fe-based compounds with hole and electron Fermi surfaces of similar sizes, where the spin fluctuations at low energies develop significantly at low temperatures. The features in the heavily electron-doped states are discussed in relation with the characteristics of the faint hole Fermi surface derived from the d_{xy} orbital that rises when h_{Pn} is high, together with the enhanced electron correlation effects.

DOI: 10.1103/PhysRevB.105.144510

I. INTRODUCTION

Superconductivity (SC) in typical iron pnictides (FePn) LaFeAsO$_{1-y}$F$_y$ ($T_c = 26$ K) [1] emerges in the vicinity of a stripe-type antiferromagnetic (AFM) order accompanied by a structural phase transition from tetragonal to orthorhombic (Ort.) phase. The parent electronic states are composed of hole and electron Fermi pockets in similar sizes. Remarkable high-T_c states have been discovered in the heavily electron-doped Fe-based compounds, such as single-layer FeSe ($T_c \geqslant 65$ K) [2,3], intercalated FeSe systems ($T_c = 30$–50 K) [4–18], and LaFeAsO$_{1-y}$(F/H)$_y$ ($T_c \sim 36$ K) [19,20]. These high-T_c states appear in the characteristic electronic states composed of large electron Fermi surface (FS) and no hole FS or the faint hole FS. Because neither the magnetic nor the orbital order phases has been reported universally in the vicinity of their SC phases, the indispensable factor for enhancing T_c is still unclear. Toward coherent understanding of many Fe-based SCs, it is important to reveal universalities and/or diversities of the SC mechanisms over a wide doping region.

Here, we focus on the reemergent high-T_c phase of heavily electron-doped 1111-compounds LaFePnO$_{1-y}$H$_y$ (Pn = As$_{1-x}$Sb$_x$, As$_{1-x'}$P$_{x'}$) [19,21–23]. As shown in Fig. 1(a), in this series the electron doping level can be broadly controlled by the content y from the lightly doped SC phase (SC1) to the reenhanced higher SC phase (SC3) in a heavily electron-doped regime [19,21–23]. The T_c within the SC3 phase is enhanced by substitution of the As site with Sb as shown in Fig. 1(b), which increases the pnictogen height (h_{Pn}) from the Fe plane [22], whereas the P substitution at the As site decreases h_{Pn} and significantly reduces T_c. Theoretically, it is expected that the variation in h_{Pn} has a significant influence on the energy level of the faint hole FS mainly from the Fe-3d_{xy} orbital [24] as shown in Fig. 1(c), which increases (decreases) when h_{Pn} becomes high (low), in addition to the electron correlation effects that are more enhanced (degraded) [25,26]. Therefore, this is a unique system to elucidate the roles of faint hole FS in the vicinity of Fermi level (E_F) in the viewpoint of the relationship between the normal electronic state and the SC state. In heavily electron-doped SC phases such as LaFeAsO$_{1-y}$(F/H)$_y$ [20,27–29] and intercalated FeSe [30–35], spin fluctuations critically enhanced at low energies have not been clearly observed in previous NMR measurements, which is in contrast to the cases of the lightly electron-doped SC states (SC1 [36] and SC2 [37,38]), where the spin fluctuations at low energies are significantly enhanced toward low temperatures. NMR study is advantageous to elucidate the evolution of the electronic states by means of a common ^{75}As nuclear probe within a same family compound from the lightly electron-doped states (SC1 and SC2) to the heavily electron-doped state (SC3).

In this study, we report systematic ^{75}As NMR studies on LaFePn(O$_{0.75}$H$_{0.25}$) for $0 \leqslant x \leqslant 0.4$ (Pn = As$_{1-x}$Sb$_x$) and $0 \leqslant x' \leqslant 0.4$ (Pn = As$_{1-x'}$P$_{x'}$), revealing that characteristic spin fluctuations suppressed at low energies appear explicitly in the Sb-substituted high-T_c compounds, whereas those are totally suppressed in P-substituted non-SC compounds. These results suggest that the contribution of the finite-energy part

---

[*] kouchi@nmr.mp.es.osaka-u.ac.jp
[†] mukuda@mp.es.osaka-u.ac.jp

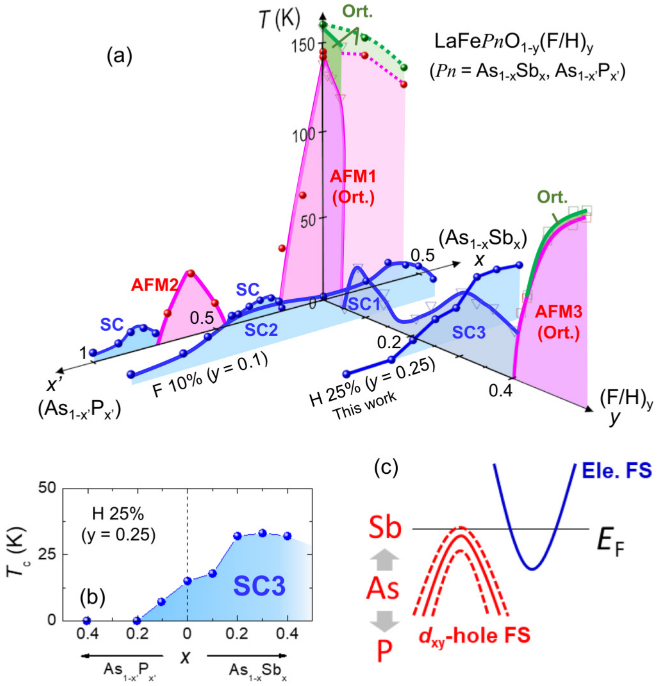

Samples	Pn site	T_c (K)	$h_{\rm Pn}$(Å)	$^{75}\nu_Q$ (MHz)
x=0.4	$\rm As_{0.6}Sb_{0.4}$	32.1	1.371	10.2
x=0.3	$\rm As_{0.7}Sb_{0.3}$	33.1	1.368	10.3
x=0.2	$\rm As_{0.8}Sb_{0.2}$	32.1	1.361	10.2
x=0	As	15.3	1.326	10.1
x'=0.2	$\rm As_{0.8}P_{0.2}$	0	1.270	9.7
x'=0.4	$\rm As_{0.6}P_{0.4}$	0	1.258	9.0

FIG. 1. (a) Phase diagram of $\mathrm{LaFe}Pn\mathrm{O}_{1-y}(\mathrm{F/H})_y$ ($Pn = \mathrm{As}_{1-x}\mathrm{Sb}_x$ and $\mathrm{As}_{1-x'}\mathrm{P}_{x'}$) for $x = 0$ [19,39], $0 \leqslant y \leqslant 0.1$ [1,21,40–47], and $y = 0.25$ [21,22]. (b) The contents (x and x') dependence of T_c for $y = 0.25$ investigated in this study [22]. (c) Schematics of possible band structure made by hole and electron Fermi surfaces around SC3. The theoretical study suggested that the d_{xy} hole FSs around (π, π) increase (reduces) by Sb substitution (P substitution) [24]. The table summarizes the properties of $\mathrm{LaFe}Pn(\mathrm{O}_{0.75}\mathrm{H}_{0.25})$ used in this study. The values of T_c and h_{Pn} are cited from the previous reports [21,22,40]. The ν_Q's at the ^{75}As site are obtained in this work.

in the spin-fluctuation spectrum may be rather important for enhancing T_c in heavily electron-doped states (SC3), which differs from that of the typical lightly doped Fe-pnictides (SC1/SC2).

II. EXPERIMENTAL

Polycrystalline samples of $\mathrm{LaFe}Pn\mathrm{O}_{0.75}\mathrm{H}_{0.25}$ with nominal contents at $0 \leqslant x \leqslant 0.4$ ($Pn = \mathrm{As}_{1-x}\mathrm{Sb}_x$) and $0 \leqslant x' \leqslant 0.4$ ($Pn = \mathrm{As}_{1-x'}\mathrm{P}_{x'}$) were synthesized using a solid state reaction method as described elsewhere [22]. Powder x-ray diffraction measurements indicate that the lattice parameters exhibit a monotonic variation with $x(x')$ [22]. The bulk T_c values were determined from an onset of zero-resistivity and diamagnetic response in dc susceptibility measurement [22,23]. As shown in Fig. 1(b), the T_c in the SC3 phase at $y = 0.25$ increases to $T_c \sim 33$ K by Sb substitution ($x \sim 0.4$), whereas the T_c decreases to zero by P substitution at $x' > 0.2$ [22]. The ^{75}As NMR measurements were performed on coarse-powder samples of $\mathrm{LaFe}Pn\mathrm{O}_{0.75}\mathrm{H}_{0.25}$ with $x = 0, 0.2, 0.3, 0.4$ ($Pn = \mathrm{As}_{1-x}\mathrm{Sb}_x$) and $x' = 0.2, 0.4$ ($Pn = \mathrm{As}_{1-x'}\mathrm{P}_{x'}$) for the fixed electron-doping level at $y = 0.25$. The Knight shift (K) was evaluated by a narrow central peak of the ^{75}As NMR spectra for the field direction of the $H_0 \perp c$ axis. The nuclear spin-lattice relaxation rate ($1/T_1$) was measured at $H_0 \sim 8$ T, which was determined by fitting a recovery curve for ^{75}As nuclear magnetization to a multiple exponential function $m(t) = 0.1\exp(-t/T_1) + 0.9\exp(-6t/T_1)$.

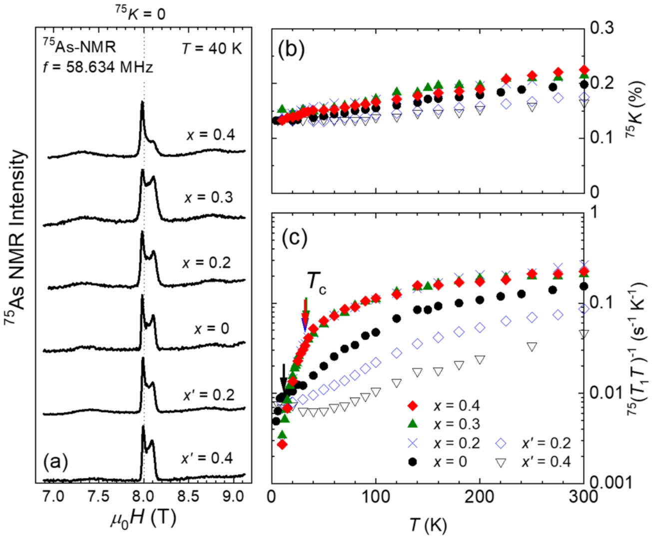

FIG. 2. (a) ^{75}As NMR spectra at $T = 40$ K for all the samples, obtained at a fixed frequency 58.634 MHz. (b) T dependence of ^{75}K in $\mathrm{LaFe}Pn\mathrm{O}_{0.75}\mathrm{H}_{0.25}$ for $0 \leqslant x \leqslant 0.4$ ($Pn = \mathrm{As}_{1-x}\mathrm{Sb}_x$) and $0 \leqslant x' \leqslant 0.4$ ($Pn = \mathrm{As}_{1-x'}\mathrm{P}_{x'}$). The ^{75}K decreases monotonically upon cooling in all the samples. (c) T dependences of $^{75}(1/T_1T)$ for each sample are more enlarged in Sb-substituted compounds, although the T dependence of ^{75}K is almost comparable.

III. RESULTS AND DISCUSSION

The ^{75}As NMR spectra of well-defined powder pattern ($I = 3/2$) were obtained for all the samples, as shown in Fig. 2(a). According to the second-order perturbation theory for the nuclear Hamiltonian with $H_0 \perp c$ [48,49], the NMR shifts consist of the Knight shift (K) and the second-order quadrupole shift, as expressed by

$$\left(\frac{f_0 - \gamma_{\rm N} H_{\rm res}}{\gamma_{\rm N} H_{\rm res}}\right) = K + \frac{3\nu_Q^2}{16(1+K)} \frac{1}{(\gamma_{\rm N} H_{\rm res})^2}, \tag{1}$$

where $\gamma_{\rm N}$ is a nuclear gyromagnetic ratio, $H_{\rm res}$ is a resonance field, and ν_Q is a nuclear quadrupole frequency at the ^{75}As site. Here, the electric field gradient asymmetry parameter (η) is assumed to be close to zero for all the samples in this study, since it was reported previously that $\eta \sim 0$ for $y < 0.3$ in heavily electron-doped $\mathrm{LaFeAsO}_{1-y}\mathrm{F}_y$ [20]. To evaluate ^{75}K and $^{75}\nu_Q$, the $H_{\rm res}$ was measured as a function of the frequency f_0. The slope in the plot of $(f_0 - \gamma_{\rm N} H_{\rm res})/\gamma_{\rm N} H_{\rm res}$ against $(\gamma_{\rm N} H_{\rm res})^{-2}$ gives an estimation of $^{75}\nu_Q$ for each

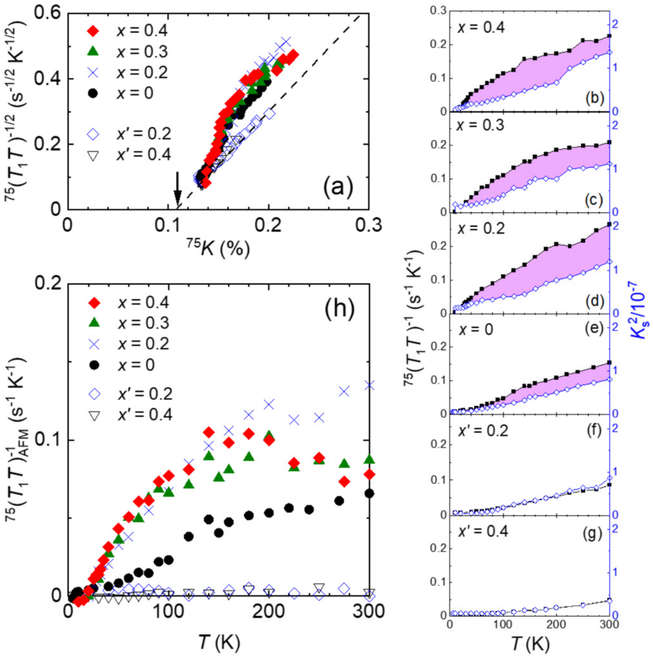

FIG. 3. (a) Plot of $^{75}(1/T_1T)^{0.5}$ vs ^{75}K for LaFePnO$_{0.75}$H$_{0.25}$ in normal states with an implicit parameter of T. It is almost linear for $x' = 0.4$, as shown by the broken line, which enables us to estimate $K_{\mathrm{chem}} \sim 0.11\%$. (b)–(g) T dependence of $^{75}(1/T_1T)$ and K_s^2. The hatched regions correspond to the component of $(1/T_1T)_{\mathrm{AFM}}$. (h) T dependence of $^{75}(1/T_1T)_{\mathrm{AFM}}$, indicating that the AFMSFs appear at high temperature but these are suppressed gradually toward low temperatures, which is more significant in $x \geqslant 0$ when the h_{Pn} is high.

sample. As summarized in the table of Fig. 1, the $^{75}\nu_Q$ is roughly in proportion to the h_{Pn}. Note that the change in $^{75}\nu_Q$ is small for $x \geqslant 0.3$, which may be due to the small change in h_{Pn} [22]. Since the $^{75}\nu_Q$ is proportional to the electric field gradient at the ^{75}As site, the result ensures the success of monotonic variation of h_{Pn} by the contents $x(x')$ from the microscopic point of view.

Figures 2(b) and 2(c) show the temperature (T) dependence of K and $^{75}(1/T_1T)$, respectively, for $0 \leqslant x \leqslant 0.4$ (Pn = As$_{1-x}$Sb$_x$) and $0 \leqslant x' \leqslant 0.4$ (Pn = As$_{1-x'}$P$_{x'}$). The ^{75}K decreases upon cooling for all the compounds, which is universal for *electron-doped* Fe-based compounds. The K comprises the spin part $K_s(T)$ and the T-independent chemical part K_{chem}, as expressed by $K(T) = K_s(T) + K_{\mathrm{chem}}$. The $K_s(T)$ is proportional to uniform susceptibility $\chi(q=0)$ with the relation $K_s(T) = A_{\mathrm{hf}}(0)\chi(q=0) \propto A_{\mathrm{hf}}(0)N(E_F)$, where $A_{\mathrm{hf}}(0)$ is the hyperfine coupling constant at $q=0$, and $N(E_F)$ is the density of states (DOS) at the Fermi level (E_F). In noncorrelated normal metals, we expect the relation $(1/T_1T) \propto N(E_F)^2$, which corresponds to the Korringa relation expressed as $(1/T_1T)^{0.5} \propto K_s$. To extract K_{chem}, the $^{75}(1/T_1T)^{0.5}$ is plotted against $^{75}K(T)$ for all the compounds, as shown in Fig. 3(a). As for $x' = 0.4$, the plot shows almost linear relation (Korringa relation) in the whole T range, indicating that the contribution of the spin fluctuations is negligibly small. It enables us to estimate K_{chem} to be $\sim 0.11\%$ for these compounds. On the other hand, in the SC compounds of $x \geqslant 0$, the deviation from the linear relation is clearly seen, indicating that the $(1/T_1T)$ includes additional contribution from the antiferromagnetic spin fluctuations (AFMSFs) at finite wave vectors.

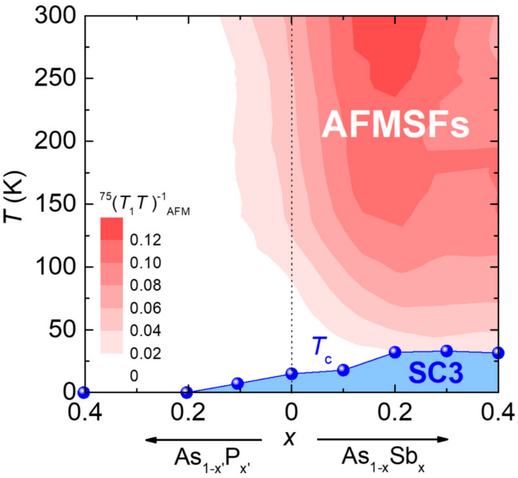

FIG. 4. Contour plot of $^{75}(1/T_1)_{\mathrm{AFM}}$ as functions of T and $x(x')$ in LaFePnO$_{1-y}$(F/H)$_y$ (Pn=As$_{1-x}$Sb$_x$ and As$_{1-x'}$P$_{x'}$). The horizontal axis also corresponds to the h_{Pn} (see the table in Fig. 1). The spin fluctuations exhibit a moderate peak at high temperatures and a suppression toward low temperatures when the h_{Pn} is high, i.e., x is large. This behavior of spin fluctuations is more significant in $x \geqslant 0$ with higher h_{Pn}, whereas it is largely suppressed in $x' \geqslant 0.2$ with low h_{Pn}, suggesting a possible relation with the reenhancement of T_c in the heavily electron-doped SC3 phase.

To extract the component derived from the AFMSFs, we assume that the $(1/T_1T)$ is decomposed as $(1/T_1T) = (1/T_1T)_{\mathrm{AFM}} + (1/T_1T)_0$, according to the previous studies [37,50–53]. The first term $(1/T_1T)_{\mathrm{AFM}}$ represents the component of AFMSFs enhanced at the finite wave vectors ($\boldsymbol{q}$) at low energies ($\omega \to 0$), which is described as

$$\left(\frac{1}{T_1T}\right)_{\mathrm{AFM}} \propto \lim_{\omega\to 0}\sum_{\boldsymbol{q}} A_{\mathrm{hf}}(\boldsymbol{q})^2\frac{\chi''(\boldsymbol{q},\omega)}{\omega}, \tag{2}$$

where $A_{\mathrm{hf}}(\boldsymbol{q})$ is the hyperfine-coupling constant at $\boldsymbol{q}$, and $\chi''(\boldsymbol{q},\omega)$ is dynamical spin susceptibility at finite wave vector $\boldsymbol{q}$ and energy ω. The second term $(1/T_1T)_0$ is the component related to $N(E_F)^2$, or $K_s^2(T)$ [$= (K - K_{\mathrm{chem}})^2$]. Figures 3(b)–3(g) show the T dependence of $^{75}(1/T_1T)$ and $K_s^2(T)$ for each sample. Since the $K_s(T)$ shows monotonous decreases upon cooling, the hatched regions in this figure correspond to the component of $(1/T_1T)_{\mathrm{AFM}}$. Consequently, the T dependence of $^{75}(1/T_1T)_{\mathrm{AFM}}$ is summarized in Fig. 3(h). We note that in the high-T_c compounds ($x \geqslant 0$) the spin fluctuations develop at the high T region moderately, but these are suppressed gradually below ~100 K. It indicates that even though the spin fluctuations are dominant in these compounds, the gaplike feature appears at low energies in the spin-fluctuation spectrum toward low temperatures.

To reveal the relationship between the h_{Pn}, the characteristics of spin fluctuations, and T_c, the contour plot of $^{75}(1/T_1T)_{\mathrm{AFM}}$ is shown in Fig. 4, as functions of content

$x(x')$ and T. The plot reveals explicitly that the spin fluctuations enhanced at high temperatures are more significant for the higher T_c compounds with higher h_{Pn} (larger x), while those are largely suppressed in non-SC compounds with lower h_{Pn} ($x' \geqslant 0.2$). It suggests that such characteristic spin fluctuations suppressed at low energies are related with the enhancement of T_c in the heavily electron-doped SC3 phase. The suppression of low-energy spin fluctuations at low temperatures was also reported in the high-T_c region of heavily electron-doped $\mathrm{LaFeAsO}_{1-y}\mathrm{F}_y$ [20], which is similar to our results. This feature differs from that of the SC1 and SC2 phases of *lightly* electron-doped La1111, where the spin fluctuations at low energies are significantly developed toward low temperatures, which has a relation with the enhancement of T_c [36,37]. The significant difference of SC3 in the heavily electron-doped regime can be attributed to the unique FS topology dominated by the enlarged electron FS and faint hole pocket. The band calculation points out that the energy level of the d_{xy} orbital that forms the faint hole pocket also increases when the h_{Pn} increases [24], which suggests a possible relation with unique spin fluctuations that appears at $x > 0$. In this FS topology, it is theoretically suggested that the finite-energy spin fluctuations give a pairing glue effectively in the heavily electron-doped SC states [54,55], even in the absence of well-nested FSs and low-energy spin fluctuations. Here we also note another important feature, that is, stronger electron correlation effect derived from the higher h_{Pn} [25,26], which is anticipated in the SC3 phase as well. In the case of heavily electron-doped $\mathrm{Ba(Fe}_{1-x}\mathrm{Co}_x)_2\mathrm{As}_2$ [50], both superconductivity and spin fluctuations disappear at $x > 0.15$, because h_{Pn} becomes *low* when Fe is replaced with Co [56]. Generally, in the unconventional SCs caused by strong correlation effects, it has been discussed theoretically that the lack of the low-energy spin fluctuations that gives rise to a pair breaking may be rather favorable [54,55,57–60]. Thus, we suggest that one possible reason for the enhanced T_c in the heavily electron-doped SC3 phase is the finite-energy spin fluctuations optimized when the FSs are not nested, if the spin fluctuations are a unique factor related to the SC mechanism.

Finally, we compare the feature of the SC3 phase with that of the lightly electron-doped SC1 and SC2 phases. It should be noted that the P substitution effect on T_c of SC3 is quite different from that in the SC1 and SC2 phases: As shown in Fig. 1(a), the SC3 phase disappears drastically by P substitution ($x' > 0.2$) while the SC1 phase is robust and the T_c is enhanced again in the SC2 phase at further P substitution [43,44,46,47]. The SC1 phase is dominated by the hole and electron FSs in similar sizes, which are mainly derived from the d_{xz}/d_{yz} orbitals, whereas the composition of the d_{xy} orbital is negligibly tiny since the h_{Pn} is low [24]. The nesting of hole and electron FSs derived mainly from d_{xz}/d_{yz} orbitals becomes better especially around the SC2/AFM2 region, which brings about the spin fluctuations at low energies developed significantly toward low temperatures [36,37,51,53,61]. It plays an indispensable role for enhancing T_c in the SC1 and SC2 phases [36,37,51,53,61]. Here, in contrast to the SC3, the contribution of the d_{xy} orbital is expected to be negligible since the energy level is far below E_F owing to the low h_{Pn}. Consequently, although spin fluctuations may be generally important for Cooper pairing in Fe-based compounds over the broad doping region, we suggest that the finite-energy component of the spin fluctuations may play an important role for enhancing the T_c in the case of the heavily electron-doped Fe-based compounds. On the other hand, in the SC3 region, it is possible that the other low-energy local fluctuations such as the orbital fluctuations could play some roles to contribute to the superconductivity, since the structural transition with the AFM3 phase appears in the vicinity of the SC3 phase. However, there is no experimental results to detect the unknown fluctuations except for spin fluctuations due to the lack of large single crystals. Further spectroscopic experiments that reveal the possible roles of orbital degrees of freedom are necessary for a general understanding of the SC mechanism in various Fe-based compounds over wide doping regions.

IV. SUMMARY

In summary, the high-T_c phase (SC3) reenhanced in the heavy electron doping on $\mathrm{LaFe}Pn\mathrm{O}_{0.75}\mathrm{H}_{0.25}$ was investigated by the common ^{75}As NMR probe by controlling the pnictogen height through the substitution at the *Pn* site. We revealed that the moderate spin fluctuations at high temperatures are gradually suppressed toward low temperatures in the high-T_c compounds with high h_{Pn}, suggesting the gaplike feature appears at low-energy regions in the spin-fluctuation spectrum toward low temperatures. This behavior is more significant when the h_{Pn} is higher in the higher T_c compounds, whereas it is more suppressed in the lower T_c compounds with lower h_{Pn}. The comparison with the theories on the FS topology suggest that the key element may be the presence of the faint hole FS derived from the d_{xy} orbital and strong correlation effects, suggesting the importance of the finite-energy AFMSFs in the heavily electron-doped states without the nested FSs. A similar phenomenon was recently reported in intercalated FeSe compounds [62] that was dominated by the large electron FS and faint hole FS or no hole FS. We suggest that this type of AFMSFs may be a characteristic feature, and one of the indispensable factors for enhancing T_c in heavily electron-doped SC states in iron-based compounds. However, in these compounds, the contribution of orbital degrees of freedom is still unclear. Further general understanding of the SC mechanism in Fe-based compounds over a broad doping region should be completed including the possible roles of orbital degrees of freedom, that should be clarified by systematic spectroscopic experiments as well as NMR probes in the future.

ACKNOWLEDGMENTS

T.K. is supported by a JSPS Fellowship (Grant No. 21J14053) and the Kato Foundation for Promotion of Science (Grant No. KS-3227). This work was supported by JSPS KAKENHI (Grants No. 16H04013 and No. 18K18734), the Murata Science Foundation, the Mitsubishi Foundation, and the Tanigawa Fund.

[1] Y. Kamihara, T. Watanabe, M. Hirano, and H. Hosono, J. Am. Chem. Soc. **130**, 3296 (2008).

[2] Q. Y. Wang, Z. Li, W. H. Zhang, Z. C. Zhang, J. S. Zhang, W. Li, H. Ding, Y. B. Ou, P. Deng, K. Chang, J. Wen, C. L. Song, K. He, J. F. Jia, S. H. Ji, Y. Y. Wang, L. L. Wang, X. Chen, X. C. Ma, and Q. K. Xue, Chin. Phys. Lett. **29**, 037402 (2012).

[3] S. He, J. He, W. Zhang, L. Zhao, D. Liu, X. Liu, D. Mou, Y. Ou, Q. Wang, Z. Li, L. Wang, Y. Peng, Y. Liu, C. Chen, L. Yu, G. Liu, X. Dong, J. Zhang, C. Chen, Z. Xu *et al.*, Nat. Mater. **12**, 605 (2013).

[4] J. Guo, S. Jin, G. Wang, S. Wang, K. Zhu, T. Zhou, M. He, and X. Chen, Phys. Rev. B **82**, 180520(R) (2010).

[5] Y. Mizuguchi, H. Takeya, Y. Kawasaki, T. Ozaki, S. Tsuda, T. Yamaguchi, and Y. Takano, Appl. Phys. Lett. **98**, 042511 (2011).

[6] A. Krzton-Maziopa, Z. Shermadini, E. Pomjakushina, V. Pomjakushin, M. Bendele, A. Amato, R. Khasanov, H. Luetkens, and K. Conder, J. Phys.: Condens. Matter **23**, 052203 (2011).

[7] A. F. Wang, J. J. Ying, Y. J. Yan, R. H. Liu, X. G. Luo, Z. Y. Li, X. F. Wang, M. Zhang, G. J. Ye, P. Cheng, Z. J. Xiang, and X. H. Chen, Phys. Rev. B **83**, 060512(R) (2011).

[8] H. D. Wang, C. H. Dong, Z. J. Li, Q. H. Mao, S. S. Zhu, C. M. Feng, H. Q. Yuan, and M. H. Fang, Europhys. Lett. **93**, 47004 (2011).

[9] M. H. Fang, H. D. Wang, C. H. Dong, Z. J. Li, C. M. Feng, J. Chen, and H. Q. Yuan, Europhys. Lett. **94**, 27009 (2011).

[10] T. P. Ying, X. L. Chen, G. Wang, S. F. Jin, T. T. Zhou, X. F. Lai, H. Zhang, and W. Y. Wang, Sci. Rep. **2**, 426 (2012).

[11] E.-W. Scheidt, V. R. Hathwar, D. Schmitz, A. Dunbar, W. Scherer, F. Mayr, V. Tsurkan, J. Deisenhofer, and A. Loidl, Eur. Phys. J. B **85**, 279 (2012).

[12] T. Hatakeda, T. Noji, T. Kawamata, M. Kato, and Y. Koike, J. Phys. Soc. Jpn. **82**, 123705 (2013).

[13] L. Zheng, M. Izumi, Y. Sakai, R. Eguchi, H. Goto, Y. Takabayashi, T. Kambe, T. Onji, S. Araki, T. C. Kobayashi, J. Kim, A. Fujiwara, and Y. Kubozono, Phys. Rev. B **88**, 094521 (2013).

[14] T. Noji, T. Hatakeda, S. Hosono, T. Kawamata, M. Kato, and Y. Koike, Physica C **504**, 8 (2014).

[15] X. F. Lu, N. Z. Wang, H. Wu, Y. P. Wu, D. Zhao, X. Z. Zeng, X. G. Luo, T. Wu, W. Bao, G. H. Zhang, F. Q. Huang, Q. Z. Huang, and X. H. Chen, Nat. Mater. **14**, 325 (2015).

[16] S. Hosono, T. Noji, T. Hatakeda, T. Kawamata, M. Kato, and Y. Koike, J. Phys. Soc. Jpn. **85**, 013702 (2016).

[17] M. Z. Shi, N. Z. Wang, B. Lei, C. Shang, F. B. Meng, L. K. Ma, F. X. Zhang, D. Z. Kuang, and X. H. Chen, Phys. Rev. Materials **2**, 074801 (2018).

[18] M. Z. Shi, N. Z. Wang, B. Lei, J. J. Ying, C. S. Zhu, Z. L. Sun, J. H. Cui, F. B. Meng, C. Shang, L. K. Ma, and X. H. Chen, New J. Phys. **20**, 123007 (2018).

[19] S. Iimura, S. Matsuishi, H. Sato, T. Hanna, Y. Muraba, S. W. Kim, J. E. Kim, M. Takata, and H. Hosono, Nat. Commun. **3**, 943 (2012).

[20] J. Yang, R. Zhou, L. L. Wei, H. X. Yang, J. Q. Li, Z. X. Zhao, and G. Q. Zheng, Chin. Phys. Lett. **32**, 107401 (2015)

[21] S. Miyasaka, M. Uekubo, H. Tsuji, M. Nakajima, S. Tajima, T. Shiota, H. Mukuda, H. Sagayama, H. Nakao, R. Kumai, and Y. Murakami, Phys. Rev. B **95**, 214515 (2017).

[22] T. Kawashima, S. Miyasaka, H. Tsuji, T. Yamamoto, M. Uekubo, A. Takemori, K. T. Lai, and S. Tajima, Sci. Rep. **11**, 10006 (2021).

[23] S. Miyasaka and S. Tajima (unpublished).

[24] K. Kuroki, H. Usui, S. Onari, R. Arita, and H. Aoki, Phys. Rev. B **79**, 224511 (2009).

[25] T. Miyake, K. Nakamura, R. Arita, and M. Imada, J. Phys. Soc. Jpn. **79**, 044705 (2010).

[26] M. Hirayama, T. Misawa, T. Miyake, and M. Imada, J. Phys. Soc. Jpn. **84**, 093703 (2015).

[27] H. Yamashita, H. Mukuda, M. Yashima, S. Furukawa, Y. Kitaoka, K. Miyazawa, P. M. Shirage, H. Eisaki, and A. Iyo, J. Phys. Soc. Jpn. **79**, 103703 (2010).

[28] N. Fujiwara, S. Tsutsumi, S. Iimura, S. Matsuishi, H. Hosono, Y. Yamakawa, and H. Kontani, Phys. Rev. Lett. **111**, 097002 (2013).

[29] R. Sakurai, N. Fujiwara, N. Kawaguchi, Y. Yamakawa, H. Kontani, S. Iimura, S. Matsuishi, and H. Hosono, Phys. Rev. B **91**, 064509 (2015).

[30] H. Kotegawa, Y. Hara, H. Nohara, H. Tou, Y. Mizuguchi, H. Takeya, and Y. Takano, J. Phys. Soc. Jpn. **80**, 043708 (2011).

[31] W. Yu, L. Ma, J. B. He, D. M. Wang, T.-L. Xia, G. F. Chen, and W. Bao, Phys. Rev. Lett. **106**, 197001 (2011).

[32] D. A. Torchetti, M. Fu, D. C. Christensen, K. J. Nelson, T. Imai, H. C. Lei, and C. Petrovic, Phys. Rev. B **83**, 104508 (2011).

[33] L. Ma, G. F. Ji, J. Zhang, J. B. He, D. M. Wang, G. F. Chen, W. Bao, and W. Yu, Phys. Rev. B **83**, 174510 (2011).

[34] Y. Texier, J. Deisenhofer, V. Tsurkan, A. Loidl, D. S. Inosov, G. Friemel, and J. Bobroff, Phys. Rev. Lett. **108**, 237002 (2012).

[35] Y. P. Wu, D. Zhao, X. R. Lian, X. F. Lu, N. Z. Wang, X. G. Luo, X. H. Chen, and T. Wu, Phys. Rev. B **91**, 125107 (2015).

[36] T. Oka, Z. Li, S. Kawasaki, G. F. Chen, N. L. Wang, and Guo-qing Zheng, Phys. Rev. Lett. **108**, 047001 (2012).

[37] T. Shiota, H. Mukuda, M. Uekubo, F. Engetsu, M. Yashima, Y. Kitaoka, K. T. Lai, H. Usui, K. Kuroki, S. Miyasaka, and S. Tajima, J. Phys. Soc. Jpn. **85**, 053706 (2016).

[38] F. Sakano, K. Nakamura, T. Kouchi, T. Shiota, F. Engetsu, K. Suzuki, R. Horikawa, M. Yashima, S. Miyasaka, S. Tajima, A. Iyo, Y.-F. Guo, K. Yamaura, E. Takayama-Muromachi, M. Yogi, and H. Mukuda, Phys. Rev. B **100**, 094509 (2019).

[39] M. Hiraishi, S. Iimura, K. M. Kojima, J. Yamaura, H. Hiraka, K. Ikeda, P. Miao, Y. Ishikawa, S. Torii, M. Miyazaki, I. Yamauchi, A. Koda, K. Ishii, M. Yoshida, J. Mizuki, R. Kadono, R. Kumai, T. Kamiyama, T. Otomo, Y. Murakami *et al.*, Nat. Phys. **10**, 300 (2014).

[40] S. J. E. Carlsson, F. Levy-Bertrand, C. Marcenat, A. Sulpice, J. Marcus, S. Pairis, T. Klein, M. Nunez-Regueiro, G. Garbarino, T. Hansen, V. Nassif, and P. Toulemonde, Phys. Rev. B **84**, 104523 (2011).

[41] H. Hosono and K. Kuroki, Phys. C (Amsterdam, Neth,) **514**, 399 (2015).

[42] H. Luetkens, H.-H. Klauss, M. Kraken, F. J. Litterst, T. Dellmann, R. Klingeler, C. Hess, R. Khasanov, A. Amato, C. Baines, M. Kosmala, O. J. Schumann, M. Braden, J. Hamann-Borrero, N. Leps, A. Kondrat, G. Behr, J. Werner, and B. Büchner, Nat. Mater. **8**, 305 (2009).

[43] S. Saijo, S. Suzuki, S. Miyasaka, and S. Tajima, Phys. C (Amsterdam, Neth.) **470**, S298 (2010).

[44] K. T. Lai, A. Takemori, S. Miyasaka, F. Engetsu, H. Mukuda, and S. Tajima, Phys. Rev. B **90**, 064504 (2014).

[45] C. Wang, S. Jiang, Q. Tao, Z. Ren, Y. Li, L. Li, C. Feng, J. Dai, G. Cao, and Z. Xu, Europhys. Lett. **86**, 47002 (2009).

[46] S. Miyasaka, A. Takemori, S. Saijo, S. Suzuki, and S. Tajima, J. Phys. Chem. Solids **72**, 414 (2011).

[47] S. Miyasaka, A. Takemori, T. Kobayashi, S. Suzuki, S. Saijo, and S. Tajima, J. Phys. Soc. Jpn. **82**, 124706 (2013).

[48] A. Abragam, *The Principles of Nuclear Magnetism* (Clarendon, Oxford, 1961).

[49] M. Takigawa, P. C. Hammel, R. H. Heffner, Z. Fisk, J. L. Smith, and R. B. Schwarz, Phys. Rev. B **39**, 300 (1989).

[50] F. L. Ning, K. Ahilan, T. Imai, A. S. Sefat, M. A. McGuire, B. C. Sales, D. Mandrus, P. Cheng, B. Shen, and H.-H. Wen, Phys. Rev. Lett. **104**, 037001 (2010).

[51] H. Mukuda, F. Engetsu, K. Yamamoto, K. T. Lai, M. Yashima, Y. Kitaoka, A. Takemori, S. Miyasaka, and S. Tajima, Phys. Rev. B **89**, 064511 (2014).

[52] M. Miyamoto, H. Mukuda, T. Kobayashi, M. Yashima, Y. Kitaoka, S. Miyasaka, and S. Tajima, Phys. Rev. B **92**, 125154 (2015).

[53] H. Mukuda, F. Engetsu, T. Shiota, K. T. Lai, M. Yashima, Y. Kitaoka, S. Miyasaka, and S. Tajima, J. Phys. Soc. Jpn. **83**, 083702 (2014).

[54] M. Nakata, D. Ogura, H. Usui, and K. Kuroki, Phys. Rev. B **95**, 214509 (2017).

[55] K. Matsumoto, D. Ogura, and K. Kuroki, J. Phys. Soc. Jpn. **89**, 044709 (2020).

[56] S. Drotziger, P. Schweiss, K. Grube, T. Wolf, P. Adelmann, C. Meingast, and H. v. Löhneysen, J. Phys. Soc. Jpn. **79**, 124705 (2010).

[57] A. J. Millis, Subir Sachdev, and C. M. Varma, Phys. Rev. B **37**, 4975 (1988).

[58] K. Kuroki and T. Higashida, and R. Arita, Phys. Rev. B **72**, 212509 (2005).

[59] K. Matsumoto, D. Ogura, and K. Kuroki, Phys. Rev. B **97**, 014516 (2018).

[60] J. P. Rodriguez, Phys. Rev. B **103**, 184513 (2021).

[61] S. Kitagawa, T. Iye, Y. Nakai, K. Ishida, C. Wang, G.-H. Cao, and Z.-A. Xu, J. Phys. Soc. Jpn. **83**, 023707 (2014).

[62] S. Nishioka, T. Kouchi, K. Suzuki, M. Yashima, H. Mukuda, M. Kodani, K. Mita, T. Kakuto, J.-H. Lee, T. Fujii, and T. Kambe, J. Phys. Soc. Jpn. **90**, 124709 (2021).